Monophenolase and Diphenolase Reaction Mechanisms of Apple and Pear Polyphenol Oxidases

Juan Carlos Espín,[†] Pedro Antonio García-Ruiz,[‡] José Tudela,[†] Ramón Varón,[§] and Francisco García-Cánovas*,[†]

GENZ (Grupo investigación Enzimología), Departamento de Bioquímica y Biología Molecular A, Facultad de Biología, Universidad de Murcia, E-30080 Murcia, Spain; Departamento de Química Orgánica, Facultad de Química, Universidad de Murcia, E-30080 Murcia, Spain; and Departamento de Química-Física, Escuela Universitaria Politécnica de Albacete, Universidad de Castilla-La Mancha, 02071 Albacete, Spain

This paper reports a quantitative study of the effect of ring substituents on the rate of monophenol hydroxylation and *o*-diphenol oxidation catalyzed by apple and pear polyphenol oxidases. A good correlation between the electronic density at the carbon atom in the 4-position of the aromatic ring for each monophenol and the V_{max} values was found. However, this correlation was not so good in the 3- and 4-positions for the *o*- diphenols assayed. NMR studies on the monophenols demonstrated the higher reactivity of 4-hydroxyanisole compared with the other monophenols assayed. Catechol was the best *o*-diphenolic substrate assayed because of the absence of a ring substituent. All of these data confirmed the proposed enzyme's reaction mechanism and indicate that the rate- limiting step in the monophenolase reaction mechanism could be the nucleophilic attack of the oxygen atom belonging to the hydroxyl group at the carbon atom in the 4-position on the copper atoms of the enzyme's active site. However, in the diphenolase reaction mechanism, the rate-limiting step could be related to both the nucleophilic attack of the oxygen atom from the hydroxyl group at the carbon atom in the 3-position on the copper atoms of the enzyme's active site and the molecular size of the substituent side chain.

Keywords: *Diphenolase; enzyme kinetics; MBTH; monophenolase; NMR; PPO*

INTRODUCTION

The enzyme polyphenol oxidase (PPO) or tyrosinase (monophenol, *o*-diphenol; oxygen oxidoreductase, EC 1.14.18.1) is of central importance in vertebrate melanin pigmentation. Enzymatic browning in vegetables and fruits is caused by the PPO activity present in plant tissues. PPO plays an important role in fruit and vegetable processing and during the storage of the processed foods. This enzyme catalyzes the hydroxylation of monophenols (monophenolase activity) and the oxidation of *o*-diphenols to *o*-quinones (diphenolase activity). The monophenolase activity of PPO is coupled to its diphenolase activity and the nonenzymatic reactions from the corresponding *o*-quinones toward melanins (Robb, 1984; Mayer and Harel, 1991; Prota, 1992; Martínez and Whitaker, 1995). The active site of PPO consists of two copper atoms and three states: "*met*" (E_m), "*deoxy*" (E_d), and "*oxy*" (E_o) (Jolley et al., 1972, 1974; Schoot-Uiterkamp and Mason, 1973; Makino and Mason, 1973; Makino et al., 1974; Schoot-Uiterkamp et al., 1976; Lerch, 1981). Structural models have been proposed for the active site of these three forms of tyrosinase (Himmelwright et al., 1980; Solomon, 1981; Wilcox et al., 1985; Solomon and Lowery, 1993; Solomon et al., 1996).

The presence of three copper states in the active site of PPO has led to a structural model being proposed for the reaction mechanism involved in the hydroxylation of monophenols and oxidation of the resulting *o*-diphenols. Monophenolic substrate initially coordinates to an axial position of one of the coppers of E_o (Wilcox et al., 1985). Rearrangement through a trigonal bipyramidal intermediate leads to the hydroxylation of monophenol by the bound peroxide, loss of H_2O, and formation of the E_mD complex (Wilcox et al., 1985; Solomon and Lowery, 1993; Solomon et al., 1996). This E_mD form can either render free diphenol to fulfill the equilibrium $E_m + D \rightleftharpoons E_mD + 2H^+$ as a first step in the diphenolase cycle or undergo oxidation of the diphenolate intermediate bound to the active site, giving a free quinone and a reduced binuclear cuprous enzyme site (E_d). *Oxy*PPO is then regenerated after the binding of molecular oxygen to E_d. The occurrence of a lag period in the monophenolase activity of PPO is related to the presence of a dead-end complex, E_mM, as has been demonstrated from kinetic studies (Rodríguez-López et al., 1992; Ros et al., 1994). The reaction mechanism of the enzyme has recently been reviewed by taking into consideration both kinetic and structural aspects (Sánchez-Ferrer et al., 1995).

The structural (Wilcox et al., 1985; Solomon and Lowery, 1993; Solomon et al., 1996) and kinetic (Rodríguez-López et al., 1992; Ros et al., 1994) mechanisms for the hydroxylation of monophenols and the oxidation of *o*-diphenols to *o*-quinones catalyzed by PPO has been established. However, the rate-limiting step in these

* Author to whom correspondence should be addressed (fax 34-68-363963; e-mail canovasf@fcu.um.es).
[†] GENZ.
[‡] Departamento de Química Orgánica.
[§] Departamento de Química-Física.

S0021-8561(97)01045-5 CCC: $15.00
Published on Web 07/01/1998

mechanisms has not been characterized due to the lack of reliable quantitative studies (Prota, 1992; Solomon et al., 1996).

The purpose of this paper is to obtain a sound kinetic and structural characterization of the monophenolase and diphenolase activities of PPO. Several monophenols and *o*-diphenols are used to study the effect of different side substituents of the benzene ring on the enzymatic reactivity of the oxygen atoms belonging to the hydroxyl groups at C-3 and C-4 (*o*-diphenols) and C-4 (monophenols). The enzymatic activity is detected spectrophotometrically by using the chromogenic nucleophile MBTH. This nucleophile traps the enzyme-generated *o*-quinones, rendering a soluble and stable MBTH-quinone adduct with high molar absorptivity. Thus, the method is highly reliable, sensitive, and precise (Winder and Harris, 1991; Rodríguez-López et al., 1994; Espín et al., 1995a,b, 1996, 1997a−e). NMR studies are carried out to establish the chemical reactivity of the oxygen atoms from the hydroxyl groups of the monophenols and *o*-diphenols tested. Thus, the chemical displacement values for C-3 and C-4 of the aromatic ring (δ_3 and δ_4, respectively) of these phenolic compounds are determined. Possible correlation between the enzymatic/chemical reactivities for the monophenols and *o*-diphenols and the enzymes (apple and pear PPOs) are studied. Furthermore, suggestions are made concerning the determination of the rate-limiting step of the monophenolase and diphenolase reaction mechanisms.

MATERIALS AND METHODS

Reagents. Catechol, DHPPA, DHPAA, dopamine, dopa methyl ester, L-dopa, 4-ethoxyphenol, 4HA, L-isoproterenol, MBTH, 4-methylcatechol, L-α-methyl dopa, phenol, PHPAA, PHPPA, TBC, L-α-methyltyrosine, and L-tyrosine were purchased from Sigma (St. Louis, MO). All other chemicals were of analytical grade and supplied by Merck (Darmstadt, Germany). Stock solutions of the phenolic substrates were prepared in 0.15 mM phosphoric acid to prevent autoxidation. The acidic character of MBTH required the use of 50 mM buffer in the assay medium. To dissolve the MBTH-quinone adducts, 2% (by vol) *N*,*N*′-dimethylformamide (DMF) was added to the assay medium (Winder and Harris, 1991; Rodríguez-López et al., 1994; Espín et al., 1995a,b, 1996, 1997a−e). Milli-Q system (Millipore Corp., Bedford, MA) ultrapure water was used throughout this research.

Triton X-114 (TX-114) was obtained from Fluka (Madrid, Spain) and condensed three times as described by Bordier (1981) but with 0.1 M PB, pH 7.3, with 20 mM EDTA. The detergent phase of the third condensation contained a concentration that ranged from 19 to 25% TX-114 (w/v).

Preparation of PPOs. PPOs from apple (var. Verdedoncella) and pear (var. Blanquilla) were extracted and partially purified by using several sequential phase partitionings with TX-114 (Espín et al., 1995a,b, 1996, 1997a).

In a routine experiment, tropolone (a specific inhibitor of PPO) was used to check the possible contamination of peroxidases or laccases in the enzymatic extract. In the presence of tropolone no activity could be detected (results not shown).

Other Methods. Protein was determined according to the method of Bradford (1976) using bovine serum albumin as standard.

Spectrophotometric Assays. Kinetic assays were carried out by measuring the appearance of the product in the reaction medium in an ultraviolet−visible Perkin-Elmer Lambda 2 spectrophotometer (Überlingen, Germany), on-line interfaced with an Intel 486 DX-66 microcomputer (Madrid, Spain). Temperature was kept at 25 °C using a Haake D1G circulating water bath (Berlin, Germany) with a heater/cooler. Reference cuvettes contained all of the components except the substrate, with a final volume of 1 mL.

Monophenolase and diphenolase activities of PPO from apple and pear were determined spectrophotometrically by using MBTH, which is a potent nucleophile through its amino group which attacks enzyme-generated *o*-quinones. This assay method is highly sensitive, reliable, and precise (Rodríguez-López et al., 1994; Espín et al., 1995a,b, 1996, 1997a). MBTH traps the enzyme-generated *o*-quinones to render a stable MBTH-quinone adduct with high molar absorptivity. The stability of the MBTH-quinone adducts and the rapidity of the kinetic assays makes this a suitable method for determining the monophenolase and diphenolase activities of PPO from several sources (Espín et al., 1995a,b, 1996, 1997a−e).

Diphenolase activity of apple and pear PPOs on catechol and 4-methylcatechol was determined by measuring the disappearance of NADH (Carlson and Miller, 1985) in short kinetic assays since MBTH-benzoquinone and MBTH-methylbenzoquinone adducts were not very soluble in the assay medium (Espín et al., 1995a, 1996).

To confirm the validity of the NADH method, several substrates (dopamine, DHPPA, and DHPAA) were assayed with both (NADH and MBTH) assay methods. The kinetic constants for the diphenolase activity of pear PPO measuring the NADH disappearance were equivalent to that determined with the MBTH method, which are summarized in Table 3.

Diphenolase activity on TBC was determined by measuring the direct formation of its enzyme-generated *o*-quinone (Waite, 1976). This substrate rendered a highly stable *o*-quinone that did not react with MBTH.

The properties of the detectable species with the different assay methods are reported in Table 1.

Kinetic Data Analysis. The K_m^D, K_m^M, V_{max}^D, and V_{max}^M values on different monophenols and *o*-diphenols were calculated from triplicate measurements of the steady-state rate, V_{ss}, for each initial substrate concentration, $[S]_0$. The reciprocals of the variances of V_{ss} were used as weighting factors in the nonlinear regression fitting of V_{ss} versus $[S]_0$ data to the Michaelis equation (Wilkinson, 1961; Endrenyi, 1981). The fitting was carried out by using Marquardt's algorithm (Marquardt, 1963) implemented in the Sigma Plot 2.01 program for Windows (Jandel Scientific, 1994). Initial estimations of K_m^D, K_m^M, V_{max}^D, and V_{max}^M were obtained from the Hanes−Woolf equation, a linear transformation of the Michaelis equation (Wilkinson, 1961).

NMR Assays. ^{13}C NMR spectra of the different monophenols and *o*-diphenols tested were obtained in a Varian Unity spectrometer of 300 MHz. The spectra were obtained at the optimum pH values for apple and pear PPOs and using ^2H_2O as solvent for the phenolic compounds. δ values were measured relative to those for tetramethylsilane ($\delta = 0$). The maximum wide line accepted in the NRM spectra was 0.06 Hz. Therefore, the maximum error accepted for each peak was ±0.03 ppm.

RESULTS AND DISCUSSION

Kinetic Assays. To gain a deeper insight into the hydroxylating and oxidation reaction mechanisms of PPO, the action of apple and pear PPOs on several monophenols and *o*-diphenols was studied. The precision and sensitivity of the assay method used to measure the monophenolase and diphenolase activities of apple and pear PPOs made it possible to determine the kinetic constants that characterize the action of PPO on the substrates assayed (Tables 2−5).

Diphenolase Activity. The speed of the catalytic action, which was directly related to the V_{max}^D values, was very dependent on the *o*-diphenol used (Tables 2 and 3). However, the affinity, which was directly related to the $1/K_m^D$ values, did not follow the same sequence as that observed for the V_{max}^D values (Tables

Table 1. Properties of the Detectable Species from Several Substrates at the Optimum pH Values of the PPOs Assayed[a]

substrate	pH	assay method	detectable species	λ_{max}	λ_i	$[MBTH]_{sat}$ (mM)	ϵ_{max} (M^{-1} cm^{-1})	ϵ_i (M^{-1} cm^{-1})
4HA	4.3	MBTH	MBTH adduct	492		0.20 ± 0.01	31300 ± 800	
	4.6			492	464	0.25 ± 0.01		26800 ± 800
4-ethoxyphenol	4.3	MBTH	MBTH adduct	488		0.20 ± 0.01	35500 ± 900	
	4.6			488	456	0.25 ± 0.01		26900 ± 800
DHPPA	4.3, 4.6	MBTH	MBTH adduct	500		1.00 ± 0.05	40000 ± 1000	
		disappearance of NADH	NADH	340			6300 ± 400	
DHPAA	4.3, 4.6	MBTH	MBTH adduct	500		1.00 ± 0.05	42600 ± 1200	
		disappearance of NADH	NADH	340			6300 ± 400	
TBC	4.3, 4.6	formation of *o*-quinone	*o*-quinone	400			1150 ± 50[b]	
dopamine	4.3, 4.6	MBTH	MBTH adduct	503		1.00 ± 0.05	42500 ± 1200	
		disappearance of NADH	NADH	340			6300 ± 400	
catechol	4.3, 4.6	disappearance of NADH	NADH	340			6300 ± 400	
4-methylcatechol	4.3, 4.6	disappearance of NADH	NADH	340			6300 ± 400	
L-dopa	4.3, 4.6	MBTH	MBTH adduct	507		3.00 ± 0.10	38000 ± 1000	
L-α-methyldopa	4.3, 4.6	MBTH	MBTH adduct	503		1.50 ± 0.08	52000 ± 2000	
dopa methyl ester	4.3, 4.6	MBTH	MBTH adduct	503		4.00 ± 0.10	52000 ± 2000	
L-isoproterenol	4.3, 4.6	MBTH	MBTH adduct	497		4.00 ± 0.10	31500 ± 1000	

[a] Conditions for calculation of ϵ were as follows: 50 mM AB (pHs 4.3, 4.6), $[MBTH]_{sat}$, 2% DMF and 300 μg/mL of PPO. Optimum pH values of apple and pear PPOs were 4.6 and 4.3, respectively. The substrate concentration was 10 μM for each substrate/PPO pair. Conditions for calculation of $[MBTH]_{sat}$ were as follows: 50 mM AB (pH 4.3, 4.6), 2% DMF, different MBTH concentrations, $5K_m$ of substrate concentration, and 50 μg/mL of the corresponding PPO. [b] Waite (1976).

Table 2. Kinetic Constants for the Diphenolase Activity of Apple PPO[a]

o-diphenol	V^D_{max} (μM/min)	K^D_m (mM)	V^D_{max}/K^D_m (min^{-1})
catechol	2210.0 ± 90.0	25.1 ± 1.0	$8.8 \times 10^{-2} \pm 7 \times 10^{-3}$
4-methylcatechol	2100.0 ± 75.0	5.5 ± 0.4	$2.0 \times 10^{-1} \pm 2 \times 10^{-2}$
DHPAA	1890.0 ± 80.1	39.8 ± 1.5	$4.7 \times 10^{-2} \pm 4 \times 10^{-3}$
DHPPA	716.0 ± 30.0	3.3 ± 0.1	$2.2 \times 10^{-1} \pm 1 \times 10^{-2}$
TBC	650.0 ± 60.1	1.5 ± 0.08	$4.3 \times 10^{-1} \pm 6 \times 10^{-2}$
dopamine	36.2 ± 2.10	1.5 ± 0.08	$2.4 \times 10^{-2} \pm 2 \times 10^{-3}$
L-dopa	3.1 ± 0.1	2.3 ± 0.1	$1.3 \times 10^{-3} \pm 1 \times 10^{-4}$
L-α-methyldopa	2.1 ± 0.1	7.2 ± 0.5	$2.8 \times 10^{-4} \pm 2 \times 10^{-5}$
dopa methyl ester	1.0 ± 0.05	1.4 ± 0.07	$7.1 \times 10^{-4} \pm 7 \times 10^{-5}$
L-isoproterenol	0.8 ± 0.04	3.1 ± 0.2	$2.6 \times 10^{-4} \pm 3 \times 10^{-5}$

[a] Conditions were as follows: AB 50 mM pH 4.6, DMF 2%, saturating MBTH concentration, and 53 μg/mL apple PPO.

Table 3. Kinetic Constants for the Diphenolase Activity of Pear PPO[a]

o-diphenol	V^D_{max} (μM/min)	K^D_m (mM)	V^D_{max}/K^D_m (min^{-1})
catechol	5100.0 ± 200.0	31.3 ± 1.8	$1.6 \times 10^{-1} \pm 1 \times 10^{-2}$
4-methylcatechol	2900.0 ± 150.0	8.1 ± 0.5	$3.6 \times 10^{-1} \pm 4 \times 10^{-2}$
DHPAA	2500.0 ± 100.0	53.1 ± 2.3	$4.7 \times 10^{-2} \pm 4 \times 10^{-3}$
DHPPA	1500.0 ± 80.0	8.8 ± 0.5	$1.7 \times 10^{-1} \pm 2 \times 10^{-2}$
TBC	1100.0 ± 80.1	3.5 ± 0.1	$3.1 \times 10^{-1} \pm 3 \times 10^{-2}$
dopamine	70.3 ± 3.0	1.5 ± 0.08	$4.6 \times 10^{-2} \pm 4 \times 10^{-3}$
L-dopa	33.1 ± 2.0	3.4 ± 0.2	$9.7 \times 10^{-3} \pm 9 \times 10^{-4}$
L-α-methyldopa	18.1 ± 1.0	1.9 ± 0.09	$9.5 \times 10^{-3} \pm 9 \times 10^{-4}$
dopa methyl ester	16.0 ± 1.0	0.9 ± 0.05	$1.8 \times 10^{-2} \pm 1 \times 10^{-3}$
L-isoproterenol	12.1 ± 1.1	3.2 ± 0.2	$3.7 \times 10^{-3} \pm 4 \times 10^{-4}$

[a] Conditions were as follows: AB 50 mM pH 4.3, DMF 2%, saturating MBTH concentration, different monophenol concentration, and 47 μg/mL pear PPO.

2, 3). The sequence obtained for the V^D_{max} values was the following: catechol > 4-methylcatechol > DHPAA > DHPPA > TBC > dopamine > L-dopa > L-α-methyldopa > dopa methyl ester > L-isoproterenol.

Monophenolase Activity. As in the case of diphenolase activity, the V^M_{max} values were very dependent on the monophenol used in a fixed sequence (Tables 4 and 5), although the K^M_m values did not follow the same sequence (Tables 4 and 5). The sequence obtained for the V^M_{max} values was the following: 4HA > 4-ethoxyphenol > PHPPA > PHPAA > tyramine. Thus, the highest catalytic velocity corresponded to the monophenols with the highest electron donor side substituent (Passi and Nazarro-Porro, 1981).

NMR Assays. To study the influence of the electron donor capacity of the side chain in C-1 toward the benzene ring, the chemical displacement values for C-3 and C-4 (δ_3 and δ_4, respectively) were determined by means of NMR assays (Tables 6 and 7) at the optimum pH values of the PPOs considered. If the side-chain

Table 4. Kinetic Constants for the Monophenolase Activity of Apple PPO[a]

monophenol	V^D_{max} (μM/min)	K^M_m (mM)	V^D_{max}/K^M_m (min^{-1})
4HA	36.1 ± 2.1	3.4 ± 0.2	$1.1 \times 10^{-2} \pm 1 \times 10^{-3}$
4-ethoxyphenol	24.9 ± 1.2	2.5 ± 0.1	$9.9 \times 10^{-3} \pm 8 \times 10^{-4}$
PHPPA	3.8 ± 0.2	2.8 ± 0.1	$1.3 \times 10^{-3} \pm 1 \times 10^{-4}$
PHPAA	1.8 ± 0.1	8.3 ± 0.5	$2.2 \times 10^{-4} \pm 2 \times 10^{-5}$
tyramine	0.2 ± 0.01	1.7 ± 0.08	$1.2 \times 10^{-4} \pm 1 \times 10^{-5}$

[a] Conditions were the same as in Table 2. The assay with phenol was not reliable because of the insolubility of the MBTH-benzoquinone adduct (Espin et al., 1995a, 1996). PPO activity could not be detected when L-tyrosine and L-α-methyltyrosine were assayed, probably due to the low catalytic constant of apple PPO toward these monophenols. This was corroborated by their high δ_4 values (Table 7).

Table 5. Kinetic Constants for the Monophenolase Activity of Pear PPO[a]

monophenol	V^D_{max} (μM/min)	K^M_m (mM)	V^D_{max}/K^M_m (min^{-1})
4HA	19.5 ± 1.1	2.6 ± 0.1	$7.5 \times 10^{-3} \pm 7 \times 10^{-4}$
4-ethoxyphenol	16.2 ± 1.2	1.9 ± 0.08	$8.5 \times 10^{-3} \pm 9 \times 10^{-4}$
PHPPA	4.1 ± 0.3	0.5 ± 0.03	$8.2 \times 10^{-3} \pm 9 \times 10^{-4}$
PHPAA	1.9 ± 0.1	2.2 ± 0.1	$8.6 \times 10^{-4} \pm 8 \times 10^{-5}$
tyramine	0.3 ± 0.01	1.7 ± 0.07	$1.8 \times 10^{-4} \pm 1 \times 10^{-5}$

[a] Conditions were the same as in Table 3. The assay with phenol was not reliable because of the insolubility of the MBTH-benzoquinone adduct (Espin et al., 1995a, 1996). PPO activity could not be detected when L-tyrosine and L-α-methyltyrosine were assayed, probably due to the low catalytic constant of pear PPO toward these monophenols. This was corroborated by their high δ_4 values (Table 7).

Scheme 1. Kinetic Reaction Mechanism for the Diphenolase Activity of PPO[a]

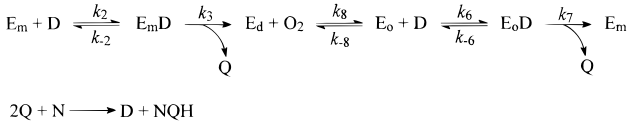

[a] E_m, *met*PPO; E_d, *deoxy*PPO; E_o, *oxy*PPO; D, diphenol; Q, *o*-quinone; N, nucleophile (MBTH); NQH, MBTH-quinone adduct.

substituent in C-1 shows a high electron donor capacity, this facilitates the transfer of the electrons toward the oxygen atom belonging to the hydroxyl group at C-4, conferring on the oxygen atom a high nucleophilic power toward the copper atoms of the enzyme's active site. Therefore, the higher the electronic density in C-3 (δ_3) and C-4 (δ_4), the higher the electronic density in the oxygen atoms belonging to the hydroxyl groups and the better nucleophile they will be.

Diphenolase Activity. The above-mentioned sequence for V^D_{max} values (Tables 2 and 3) could be explained by the overall effect of the values of δ_3 and δ_4 (Table 6) and the molecular size of the side substituent chain in C-1. In the different *o*-diphenols assayed, it should be noted that $\delta_3 > \delta_4$ (Table 6). In other words, the nucleophilic capacity of the OH group at C-4 is higher than that at C-3, and so the attack on the part of the oxygen atom from the OH group at C-3 could be the limiting step in the reaction mechanism. However, the fact that the substrate binds to the copper atoms of the active site might result in a distortion, which could in turn provoke electronic, steric, or hydrophobic effects of the side substituent on the different amino acids of the active site (Scheme 1).

All of the *o*-diphenols assayed were good nucleophiles (low δ_3 and δ_4 values) when were compared with monophenols (high δ_4 values) (Tables 6 and 7). The *o*-diphenols with low molecular size substituent side chain were very good substrates. That was the case of catechol with higher δ_3 values than those for other *o*-diphenols but with no substituent side chain. The absence of steric hindrance in the action of PPO on catechol led to this substrate being the best *o*-diphenol assayed (Tables 2 and 3). The same case was observed when DHPAA was compared with DHPPA and when dopamine was compared with L-dopa and L-α-methyldopa, as well as when dopa methyl ester was compared with L-isoproterenol.

On the other hand, *o*-diphenols with lower δ_3 (better nucleophiles) than those for other *o*-diphenols were not very good substrates because of the high molecular size of their side substituent chain. That was the case of TBC, which despite its δ_3 value (the lowest value in Table 6), was assorted in fifth position regarding its reactivity. The same case was observed when L-α-methyldopa was compared with dopamine and L-dopa, as well as when L-isoproterenol was compared with dopa methyl ester.

Furthermore, the preference in reactivity of PPO toward *o*-diphenols with similar δ_3 values might be also combined with the contribution of low δ_4 values. That was the case of the catecholamines assayed (Table 6, from dopamine to L-isoproterenol).

Monophenolase Activity. As in the case of the *o*-diphenols, a side substituent with a high electron donor capacity in the monophenolic substrates facilitated their transfer toward the oxygen atom from the hydroxyl group at C-4 (Passi and Nazarro-Porro, 1981). However, the side substituent did not affect C-3, which meant that the nucleophilic power of the oxygen atom at C-4 on the copper atoms of the enzyme's active site was high. NMR assays predicted the highest reactivity for 4HA (Table 7). This high nucleophilic power was corroborated by kinetic assays using apple and pear PPOs (Tables 4 and 5).

Table 6. δ_3 and δ_4 Values for C-3 and C-4, Respectively, of the Aromatic Ring of *o*-Diphenols at pH 4.5[a]

o-diphenol	δ_3 (ppm)	δ_4 (ppm)	*o*-diphenol	δ_3 (ppm)	δ_4 (ppm)
catechol	146.59	146.59	dopamine	146.86	145.66
4-methylcatechol	146.43	144.06	L-dopa	146.83	145.98
DHPAA	146.59	145.51	L-α-methyldopa	146.67	146.13
DHPPA	146.58	144.85	dopa methyl ester	146.90	146.18
TBC	146.24	144.07	L-isoproterenol	146.88	146.83

[a] Conditions were as follows: saturating *o*-diphenol concentration in ^2H_2O at pH 4.5. δ values were measured relative to those for tetramethylsilane ($\delta = 0$). The maximum wide line accepted in the NRM spectra was 0.06 Hz. Therefore, the maximum accepted error for each peak was ± 0.03 ppm.

Table 7. δ_3 and δ_4 Values for C-3 and C-4, Respectively, of the Aromatic Ring of Monophenols at pH 4.5[a]

monophenol	δ_3 (ppm)	δ_4 (ppm)	monophenol	δ_3 (ppm)	δ_4 (ppm)
4HA	118.86	152.25	tyramine	118.51	157.27
4-ethoxyphenol	119.01	152.39	phenol	118.13	158.15
PHPPA	118.07	156.23	L-tyrosine	118.08	159.32
PHPAA	118.18	156.85	L-α-methyltyrosine	118.11	159.54

[a] Conditions were as follows: saturating monophenol concentration in ^2H_2O at pH 4.5. δ values were measured relative to those for tetramethylsilane ($\delta = 0$). The maximum wide line accepted in the NRM spectra was 0.06 Hz. Therefore, the maximum accepted error for each peak was ± 0.03 ppm.

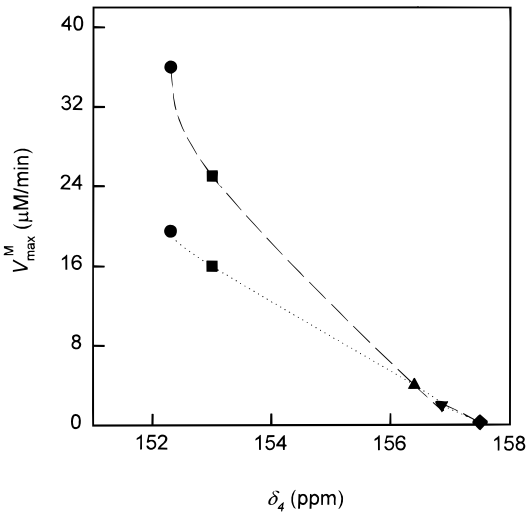

Figure 1. Dependence of V^M_{max} data vs δ_4 values at pH 4.6 and 4.3 in the monophenolase activity of apple (—) and pear (···) PPOs, respectively: (●) 4HA; (■) 4-ethoxyphenol; (▲) PHPPA; (▼) PHPAA; (◆) tyramine. Spectrophotometric assays: 50 mM AB pH 4.6 and 4.3 (apple and pear PPOs, respectively); 2% DMF; saturating MBTH concentration for each monophenol; 53 μg/mL apple PPO and 47 μg/mL pear PPO. NMR assays for determining δ_4: saturating monophenol concentration in ^2H_2O at pH 4.5. δ values were measured relative to those for tetramethylsilane ($\delta = 0$).

There was a good correlation between the enzymatic and nonenzymatic reactivities as represented by the high V^M_{max} value and low δ_4 value, respectively (Figure 1). The size of the substituent side chain was not significant mainly due to the low nucleophilic power of the monophenols. Moreover, if the rate-limiting step was the electrophilic attack on C-3, since the δ_3 values were almost similar (Table 7), the V^M_{max} values should have been the same, but this was not the case. For this reason, the nucleophilic attack of the oxygen atom from the monophenolic hydroxyl group on the active site of PPO might be the rate-limiting step in the monophenolase reaction mechanism of PPO.

Kinetic Reaction Mechanism. *Diphenolase Activity*. The diphenolase activity reaction mechanism of PPO is a lineal system (Scheme 2) involving several rate constants that lead to the following expressions for V^D_{max} and K^D_m (Rodríguez-López et al., 1992; Ros et al., 1994):

$$V^D_{max} = k_3k_7[E]_0/(k_3 + k_7) \quad (1)$$

$$K^D_m = [k_2k_3(k_{-6} + k_7) + k_6k_7(k_{-2} + k_3)]/k_2k_6(k_3 + k_7) \quad (2)$$

The V^D_{max} expression involves only rate constants that rule transformation steps in the reaction mechanism, whereas the K^D_m expression involves kinetic constants that rule both transformation and binding steps in the same reaction mechanism.

Considering eq 1, V^D_{max} expression is directly dependent on the rate constants k_3 and k_7. However, K^D_m is not directly dependent on this kinetic constant (eq 2). Therefore, in the expressions for V^D_{max} and K^D_m, any increase in the values of k_3 and k_7 will result in an

Scheme 2. Structural Reaction Mechanism for the Diphenolase Activity of PPO[a]

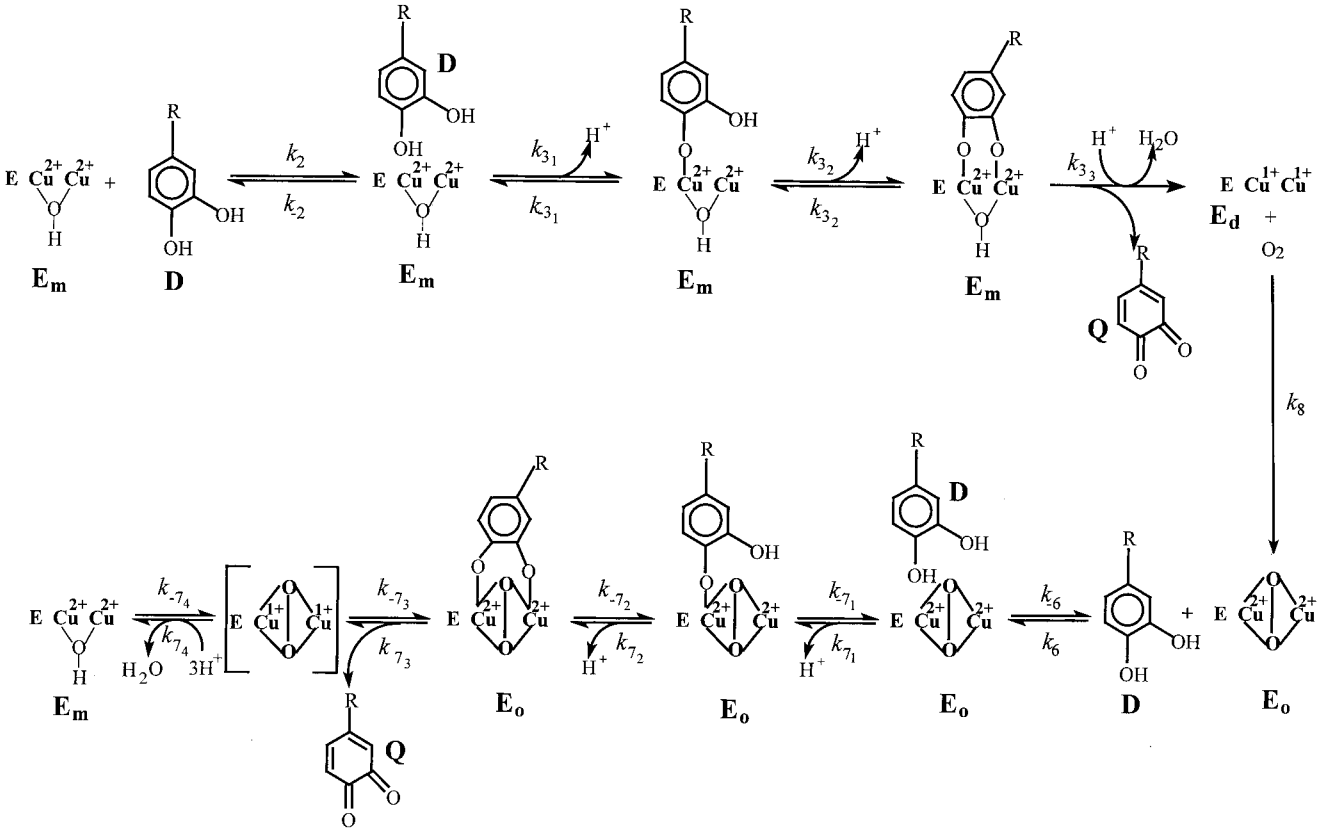

[a] E_m, ($ECu^{2+}Cu^{2+}$, *met*PPO); E_d, ($ECu^{+}Cu^{+}$, *deoxy*PPO); E_o, (ECu^{2+}-O_2^{2-}-Cu^{2+}, *oxy*PPO); D, *o*-diphenol; Q, *o*-quinone. [The numeric notation of the rate constants is an extension of that previously used in Rodríguez-López et al. (1992).]

Scheme 3. Kinetic Reaction Mechanism of PPO on Monophenols and *o*-Diphenols Coupled to Nonenzymatic Reactions from *o*-quinone[a]

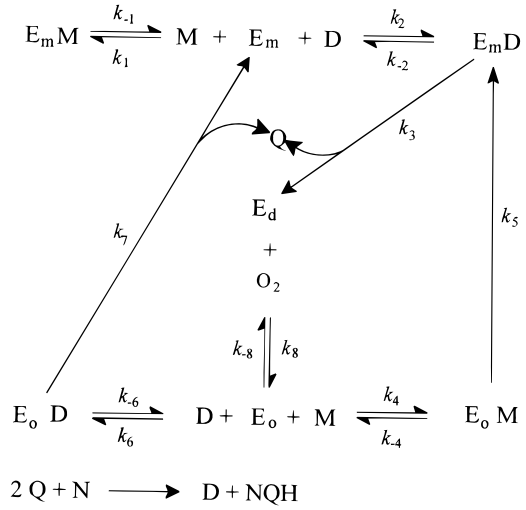

[a] E_m, *met*PPO; E_d, *deoxy*PPO; E_o, *oxy*PPO; M, monophenol; D, diphenol; Q, *o*-quinone; N, nucleophile (MBTH); NQH, MBTH-quinone adduct.

increase in V^D_{max}, but not in K^D_m. It is possible that a side chain with very low molecular size (such as catechol) or one with a high electron donor capacity (such as 4-methylcatechol) could cause such an increase in the k_3 and k_7 values with a subsequent increase in the V^D_{max} value.

Monophenolase Activity. The monophenolase reaction mechanism of PPO is a cyclic system (Scheme 3) involving many kinetic constants and giving rise to complex expressions for V^M_{max} and K^M_m (Rodríguez-López et al., 1992; Ros et al., 1994):

$$V^M_{max} = [2K_1k_2k_3k_4k_5k_6k_7(k_{-4} + k_5)(k_{-6} + k_7)/ K_1k_2k_4k_5k_6(k_3 + 3k_7)(k_{-4} + k_5)(k_{-6} + k_7) + 2k_6k_7(k_{-4} + k_5)[K_1k_2k_3k_4(k_{-6} + k_7) + k_6k_7(3k_{-2} + k_3)(k_{-4} + k_5)]][E]_0 \quad (3)$$

$$K^M_m = 2K_1k_6k_7(k_{-4} + k_5)^2[k_2k_3(k_{-6} + k_7) + k_6k_7(3k_{-2} + k_3)]/ K_1k_2k_4k_5k_6(k_3 + 3k_7)(k_{-4} + k_5)(k_{-6} + k_7) + 2k_6k_7(k_{-4} + k_5)[K_1k_2k_3k_4(k_{-6} + k_7) + k_6k_7(3k_{-2} + k_3)(k_{-4} + k_5)] \quad (4)$$

In a previous work the possible limiting step in the monophenolase activity of PPO was discussed (Ros et al., 1994). The quantitative relation between the *o*-diphenol accumulated in the steady state ($[D]_{ss}$) and the initial monophenol concentration ($[M]_0$) was established ($[D]_{ss}/[M]_0$). This relation was designated **R** (relation parameter), and its analytical expression was $\mathbf{R} = {}^1/_2(k_5/k_7)/K^D_o/K^M_o$). On the basis of the experimental determination of the low **R** values for several monophenol/*o*-diphenol pairs, the step ruled by k_5 (hydroxylation reaction) was proposed as the rate-limiting step in the monophenolase reaction of PPO (Scheme 3) (Ros et al., 1994). It is of note that V^M_{max} is directly dependent on the value of the hydroxylation constant (k_5), although K^M_m is not because k_5 is in the denominator as an adding term. Considering eq 3 and 4, an increase in k_5 will cause an increase in V^M_{max}, but not in K^M_m. The results shown in Tables 4 and 5 confirm the predictions of the NMR studies (Table 7) for the action of apple and pear PPOs on the different monophenols assayed. Thus, the monophenol with the highest nucleophilic power of the oxygen atom belonging to the hydroxyl group at C-4 will show the highest V^M_{max} value. The following step, the electrophilic attack on C-3, is not the rate- limiting step because V^M_{max} values were assorted according to δ_4 values. In this case, the effect of the molecular size of the side chain is not significant due to the slowness of the nucleophilic attack of the oxygen atom from the OH group of monophenols on the copper atoms of the enzyme's active site.

Structural Reaction Mechanism. A structural reaction mechanism of PPO has been proposed by Dr. Solomon's research group (Wilcox et al., 1985; Solomon and Lowery, 1993; Solomon et al., 1996).

Diphenolase Activity. The experimental results described in this paper are in accordance with the kinetic reaction mechanism previously proposed by our research group (Rodríguez-López et al., 1992; Ros et al., 1994). However, the kinetic steps ruled by k_3 [$E_mD \rightarrow$ (k_3) E_d + Q] and k_7 [$E_oD \rightarrow$ (k_7) E_m + Q] could involve several substeps from a structural point of view, 3_1, 3_2, and 3_3 and 7_1, 7_2, 7_3, and 7_4, respectively (Schemes 1 and 2). After the binding of the *o*-diphenol to the forms of the enzyme with no covalent interactions (Scheme 2, steps 2 and 6), the nucleophilic attack of the hydroxyl groups from C-4 and C-3 would take place and the final process would involve oxidoreduction. From the experimental results obtained (V^D_{max} and NMR values) it might be suggested that the rate-limiting step corresponds to the nucleophilic attack of the oxygen atom from the hydroxyl group at C-3 (Scheme 2, steps 3_2 and 7_2). According to the data of Table 6, the nucleophilic power at C-3 was lower than that at C-4 ($\delta_3 > \delta_4$). Moreover, little differences were found in the δ_3 values, which supported the significant effect of the side-chain substituent. For example, TBC should be the best *o*-diphenol assayed because it had the lowest δ_3 value. However, TBC was not the best *o*-diphenol because of the molecular size of its side chain. The same could be observed in the case of catechol and 4-methylcatechol and L-dopa and L-α-methyldopa. In the above reaction mechanism, the molecular size of the side chain might have assumed greater significance after the nucleophilic attack had taken place.

Monophenolase Activity. The experimental results previously described agree with a kinetic reaction mechanism previously proposed (Rodríguez-López et al., 1992; Ros et al., 1994) (Scheme 3). However, the kinetic step ruled by k_5, $E_{oM} \rightarrow$ (k_5) E_mD, could involve several substeps from a structural point of view (5_1 and 5_2) (Scheme 4). The nucleophilic attack of the oxygen atom from the OH group of M to E_o would result in the formation of E_oM, which would give rise to an intermediate covalent species, E_o−M. This process could be responsible for the rate of the overall kinetic step ruled by k_5 (Scheme 4). Table 7 shows high δ_4 values (low nucleophilic power) for monophenols. Moreover, there were significant differences in the δ_4 values depending on the capacity of the side-chain substituent to donate electrons to the aromatic ring. δ_3 values were low due to the absence of a hydroxyl group. Therefore, according to the experimental V^M_{max} and NMR values obtained, it might be suggested that the rate-limiting step in the

Scheme 4. Structural Model for the Enzyme's Reaction Mechanism on Monophenols[a]

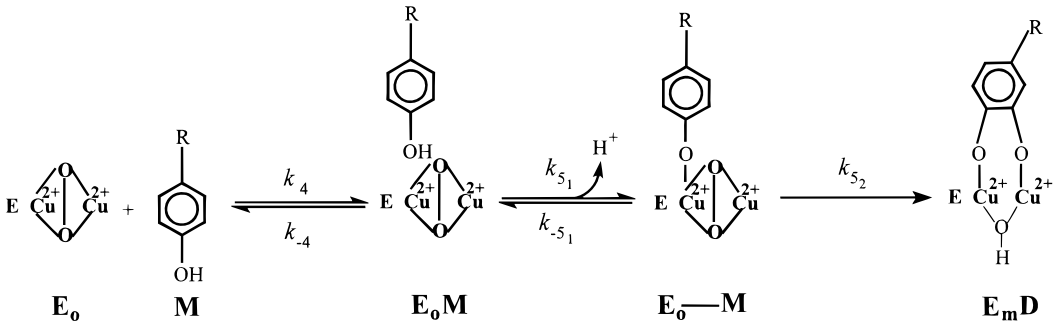

[a] E_m, *met*PPO; E_o, *oxy*PPO; M, monophenol; D, *o*-diphenol. [The numeric notation of the rate constants is an extension of that previously used in Rodríguez-López et al. (1992).]

monophenolase reaction mechanism is the nucleophilic attack of the oxygen atom belonging to the hydroxyl group at C-4 on the copper atoms of the enzyme's active site (Scheme 4, step 5_1). In the case of monophenols, the size of the side-chain substituent (steric effect) is not significant but its capacity to donate electrons to the aromatic ring (electronic effect) is.

To sum up, the ring substituent in C-1 for the different monophenols and *o*-diphenols assayed was of great importance for explaining the catalytic rapidity (V_{max}) of PPO in the reaction mechanism. All of the *o*-diphenols assayed were good nucleophiles (low δ_3 and δ_4 values). Therefore, the influence of this side chain in C-1 on the nucleophilic power of the oxygen atom from the hydroxyl group at C-4 was not very significant. For *o*-diphenols the molecular size of this side chain in C-1 assumed greater importance on V^D_{max} (steric effect). In the case of monophenols, the side chain in C-1 had a strong effect on the nucleophilic power of the oxygen atom from the hydroxyl group at C-4 (electronic effect). Monophenols were poor nucleophiles (high δ_4 values), which meant that the reaction was so slow (rate-limiting) that the effect of the size of the side chain was not significant on V^M_{max}.

ABBREVIATIONS USED

AB, sodium acetate buffer; C-1, carbon atom in the 1-position of the benzene ring; C-3, carbon atom in the 3-position of the benzene ring; C-4, carbon atom in the 4-position of the benzene ring; D, *o*-diphenol; ^2H_2O, deuterium oxide (heavy water); $[D]_0$, initial *o*-diphenol concentration; $[D]_{ss}$, *o*-diphenol concentration in the steady state; DMF, *N*,*N*′-dimethylformamide; δ_3, chemical displacement value for C-3; δ_4, chemical displacement value for C-4; DHPAA, 3,4-dihydroxyphenylacetic acid; DHPPA, 3,4-dihydroxyphenylpropionic acid; E_d, reduced form of polyphenol oxidase with Cu^+—Cu^+ in the active site; E_m, *met*polyphenol oxidase with Cu^{2+}—Cu^{2+} in the active site; E_o, *oxy*polyphenol oxidase with Cu^{2+}—O_2^{2-}—Cu^{2+} in the active site; 4HA, 4-hydroxyanisole; λ_{max}, wavelength at the maximum of absorbance; λ_i, wavelength at the isosbestic point; K^D_o, Michaelis constant of *oxy*PPO toward *o*-diphenols; K^M_o, apparent Michaelis constant of *oxy*PPO toward monophenols; K^D_o, apparent Michaelis constant of *oxy*PPO toward *o*-diphenols; K^M_m, apparent Michaelis constant of PPO toward monophenols; M, monophenol; $[M]_0$, initial monophenol concentration; MBTH, 3-methyl- 2-benzothiazolinone hydrazone; $[MBTH]_{sat}$, saturating MBTH concentration; NADH, reduced nicotinamine adenine dinucleotide; NMR, nuclear magnetic resonance; PB, sodium phosphate buffer; PHPAA, *p*-hydroxyphenylacetic acid; PHPPA, *p*- hydroxyphenylpropionic acid; $[S]_0$, initial substrate concentration; TBC, 4-*tert*- butylcatechol; V_{ss}, steady-state rate; V^D_{max}, maximum steady-state rate of PPO toward *o*-diphenols; V^M_{max}, maximum steady-state rate of PPO toward monophenols.

LITERATURE CITED

Bordier, C. Phase separation of integral membrane proteins in Triton X-114 solution. *J. Biol. Chem.* **1981**, *256*, 1604−1607.

Carlson, B. W.; Miller, L. Mechanism of the oxidation of NADH by quinones. Energetics of one-electron and hydride routes. *J. Am. Chem. Soc.* **1985**, *107*, 479−485.

Endrenyi, L. *Kinetic Data Analysis: Design and Analysis of Enzyme and Pharmacokinetics Experiments*; Plenum Press: New York, 1981.

Espín, J. C.; Morales, M.; Varón, R.; Tudela, J.; García-Cánovas, F. A continuous spectrophotometric method for determining the monophenolase and diphenolase activities of apple polyphenol oxidase. *Anal. Biochem.* **1995a**, *231*, 237−246.

Espín, J. C.; Morales, M.; Varón, R.; Tudela, J.; García-Cánovas, F. Monophenolase activity of polyphenol oxidase from Verdedoncella apple. *J. Agric. Food Chem.* **1995b**, *43*, 2807−2812.

Espín, J. C.; Morales, M.; Varón, R.; Tudela, J.; García-Cánovas, F. Continuous spectrophotometric method for determining monophenolase and diphenolase activities of pear polyphenol oxidase. *J. Food Sci.* **1996**, *61*, 1177−1201.

Espín, J. C.; Morales, M.; Varón, R.; Tudela, J.; García-Cánovas, F. Monophenolase activity of polyphenol oxidase from Blanquilla pear. *Phytochemistry* **1997a**, *44*, 17−22.

Espín, J. C.; Morales, M.; García-Ruiz, P. A.; Tudela, J.; García-Cánovas, F. Improvement of a continuous spectrophotometric method for determining the monophenolase and diphenolase activities of mushroom polyphenol oxidase. *J. Agric. Food Chem.* **1997b**, *45*, 1084−1090.

Espín, J. C.; Trujano, M. F.; Tudela, J.; García-Cánovas, F. Monophenolase activity of polyphenol oxidase from Haas avocado. *J. Agric. Food Chem.* **1997c**, *45*, 1091−1096.

Espín, J. C.; Ochoa, M.; Tudela, J.; García-Cánovas, F. Monophenolase activity of strawberry polyphenol oxidase. *Phytochemistry* **1997d**, *45*, 667−670.

Espín, J. C.; Varón, R.; Tudela, J.; García-Cánovas, F. Kinetic study of the oxidation of 4- hydroxyanisole catalyzed by tyrosinase. *Biochem. Mol. Biol. Intact.* **1997e**, *41*, 1265−1276.

Himmelwright, R. S.; Eickman, N. C.; Lu Bien, C. D.; Lerch, K.; Solomon, E. I. Chemical and spectroscopic studies of the binuclear copper active site of Neurospora tyrosinase: comparison to hemocyanins. *J. Am. Chem. Soc.* **1980**, *102*, 7339−7344.

Jandel Scientific. *Sigma Plot 2.01 for Windows*; Jandel Scientific: Corte Madera, CA, 1994.

Jolley, R. L., Jr.; Evans, L. H.; Mason, H. S. Reversible oxygenation of tyrosinase. *Biochem. Biophys. Res. Commun.* **1972**, *46*, 878−884.

Jolley, R. L., Jr.; Evans, L. H.; Makino, N.; Mason, H. S. *J. Biol. Chem.* **1974**, *249*, 335−345.

Lerch, K. *Metal Ions in Biological Systems*; Sigel, H., Ed.; Marcel Dekker: New York, 1981; Vol. 13. pp 143−186.

Makino, N.; Mason, H. S. Reactivity of oxytyrosinase toward substrates. *J. Biol. Chem.* **1973**, *248*, 5731−5735.

Makino, N.; McMahill, P.; Mason, H. S. The oxidation state of copper in resting tyrosinase. *J. Biol. Chem.* **1974**, *249*, 6062−6066.

Marquardt, D. An algorithm for least-squares estimation of nonlinear parameters. *J. Soc. Ind. Appl. Math.* **1963**, *11*, 431−441.

Martínez, M. V.; Whitaker, J. R. The biochemistry and control of enzymatic browning. *Trends Food Sci. Technol.* **1995**, *6*, 195−200.

Mayer, A. M.; Harel, E. Polyphenoloxidases and their significance in fruits and vegetables. In *Food Enzymology*; Fox, P. F., Ed.; Elsevier: London, 1991; pp 373−379.

Passi, S.; Nazarro-Porro, M. Molecular basis of substrate and inhibitory specificity of tyrosinase: phenolic compounds. *Br. J. Dermatol.* **1981**, *104*, 659−665.

Prota, G. *Melanins and Melanogenesis*; Jovanovich, H. B., Ed.; Academic Press: San Diego, CA, 1992.

Robb, D. A. Tyrosinase. In *Copper Proteins and Copper Enzymes*; Lontie, R., Ed.; CRC Press: Boca Raton, FL, 1984; pp 207−241.

Rodríguez-López, J. N.; Tudela, J.; Varón, R.; García-Carmona, F.; García-Cánovas, F. Analysis of a kinetic model for melanin biosynthesis pathway. *J. Biol. Chem.* **1992**, *267*, 3801−3810.

Rodríguez-López, J. N.; Escribano, J.; García-Cánovas, F. A continuous spectrophotometric method for the determination of monophenolase activity of tyrosinase using 3-methyl-2- benzothiazolinone hydrazone. *Anal. Biochem.* **1994**, *216*, 205−212.

Ros, J. R.; Rodríguez-López, J. N.; García-Cánovas, F. Tyrosinase: Kinetic analysis of the transient phase and the steady state. *Biochim. Biophys. Acta* **1994**, *1204*, 33−42.

Sánchez-Ferrer, A.; Rodríguez-López, J. N.; García-Cánovas, F.; García-Carmona, F. Tyrosinase: A comprehensive review of its mechanism. *Biochim. Biophys. Acta* **1995**, *1247*, 1−11.

Schoot-Uiterkamp, A. J. M.; Mason, H. S. Magnetic dipole−dipole coupled Cu(II) pairs in nitric oxide-treated tyrosinase: a structural relationship between the active sites of tyrosinase and hemocyanin. *Proc. Natl. Acad. Sci. U.S.A.* **1973**, *70*, 993−996.

Schoot-Uiterkamp, A. J. M.; Evans, L. H.; Jolley, R. L.; Mason, H. S. Absorption and circular dichroism spectra of different forms of mushroom tyrosinase. *Biochim. Biophys. Acta* **1976**, *453*, 200−204.

Solomon, E. I. In *Copper Proteins and Copper Enzymes*; Spiro, T. G., Ed.; Wiley-Interscience: New York, 1981; Vol. III, pp 41−108.

Solomon, E. I.; Lowery, M. D. Electronic structure contributions to function in bioinorganic chemistry *Science* **1993**, *259*, 1575−1581.

Solomon, E. I.; Sundaram, U. M.; Machonkin, T. E. Multicopper oxidases and oxygenases. *Chem. Rev.* **1996**, *96*, 2563−2605.

Waite, J. H. Calculating extinction coefficients for enzymatically produced *o*-quinones. *Anal. Biochem.* **1976**, *75*, 211−218.

Wilcox, D. E.; Porras, A. G.; Hwang, Y. T.; Lerch, K.; Winkler, M. E.; Solomon, E. I. Substrate analogue binding to the coupled binuclear copper active site in tyrosinase. *J. Am. Chem. Soc.* **1985**, *107*, 4015−4027.

Wilkinson, G. N. Statistical estimations in enzyme kinetics. *Biochem. J.* **1961**, *80*, 324−332.

Winder, A. J.; Harris, H. New assays for the tyrosine hydroxylase and dopa oxidase activities of tyrosinase. *Eur. J. Biochem.* **1991**, *198*, 317−326.

Received for review December 8, 1997. Revised manuscript received April 20, 1998. Accepted April 29, 1998. This study was partially supported by Comisión Interministerial de Ciencia y Tecnología, Project CICYT ALI96-1111-C04. J.C.E. has a fellowship from the Programa Nacional de Formación del Personal Investigador, Ministerio de Educación y Ciencia (Spain), Reference AP93 34785457.

JF971045V